SHEAR FAILURE OF REINFORCED CONCRETE COLUMNS DUE TO BIAXIAL LATERAL FORCES

O. Joh (I)
T. Shibata (II)
Presenting Author: O. Joh

SUMMARY

The investigation deals with the shear strength and the deformability of reinforced concrete columns under biaxial lateral forces. Nine specimens with a square cross section and four specimens with a rectangular cross section were subjected to lateral displacement reversals with increasing amplitude in the direction perpendicular or oblique to an axis of cross section. The normalized interaction curves relating to the shear components in the directions of both the principal axes of cross section may be expressed with circle at ultimate shear strength as well as at initial shear cracking.

INTRODUCTION

Several design criteria for columns under axial load and biaxial bending have already presented and the interaction diagrams for square columns are available in the ACI handbook. On the other hand, the data on the behavior of the columns failed in shear under biaxial lateral forces are scarcely accumulated. In the present paper, the interaction curves for shear strength and the biaxial lateral force-deformation relationship of short columns with square or rectangular cross section are discussed on the basis of the data from tests of 13 specimens.

TEST PROGRAM

Test Specimens. Principal variables in the test program were: (1) shape of cross section of column, (2) axial load ratio: $\eta = P/bhf'_c$ and (3) angle of lateral loading direction from the axis of cross section. The test specimens consisted of 9 columns with a 30 x 30 cm square cross section and 4 columns with a 22.5 x 40 cm rectangular cross section. The variations of the specimens are shown in Table 1. For the whole specimens the cross sectional area was 900 cm^2 and the unsupported height of column was 90 cm. Every specimen had the loading stubs on the top and the bottom of column as shown in Fig.1. The longitudinal reinforcement was provided with 8 deformed bars of 19 mm (2.25 % in gross reinforcement ratio) for every column. Shear reinforcement ratios were varied from 0.284% to 0.337% so as to arrange the strength against shear to be about 70 % of the strength against bending in the whole cases. The dimensions of the specimens are shown in Table 2. The concrete strength corresponding to each specimen is presented in Table 4. The average strength of concrete was 274 kg/cm^2. The properties of reinforcement bars are summarized in Table 3.

Loading Method. The loading arrangement is schematically shown in Fig. 2. The bottom stub was clamped in the lower steel beam which was fixed on the

(I) Associate Professor of Structural Engineering, Hokkaido University, Sapporo/Japan
(II) Professor of Structural Engineering, Hokkaido University, Sapporo/Japan

floor and the top stub was restrained with upper clamping steel beam which was set up to move freely on horizontal planes parallel to the floor by connecting to the lower beam with four tie-rods. The lateral force was applied with a hydraulic actuator attached to the upper beam through universal joints. The axial load was applied with a hydraulic jack through four sets of tie-bar and spring, independently of the lateral loading setup. Coupled teflon sheets were inserted between the contacted faces of the upper stub and the clamping steel beam so as to diminish the friction between them and to minimize the fluctuation of the axial stress in the column due to the length change in the large deformation region. Consequently the axial stress in the columns was almost constant through the test. Lateral loading was controlled with relative displacement between the vertical axes of the upper stub and the lower stub. The amplitude of lateral displacement reversals was increased by following the geometric progression series as expressed in $R = 1.5 \times 1.2^{n-1} \times 10^{-3}$ rad. where R = rotation of column in the clear height and n = number of cycle.

Measurement. Load cells were used to measure the applied shear, axial load and the vertical reactions at the ends of the upper clamping beam. Differential transformers were used to measure the relative displacement between the axes of the stubs and length change of column during the test. The strains in the longitudinal and transverse reinforcement at several locations shown in Fig. 1 were measured with pairs of high-elongation strain gages.

PROCESS OF CRACKING AND FAILURE

All the columns resulted in shear failure at the ultimate stage. The crack patterns in all the columns at the end of test are shown in Fig. 3, where the cracks which occurred in every reversing stage of half-cycle are excepted for legibility. The illustration for cracks in the column subjected to biaxial lateral loading is expressed as a projection on the plane which includes the elastically calculated locus of the longitudinal axis of column under the lateral force. Fig. 4 shows examples of the typical cracks at early stages and the conspicuous cracks at ultimate stages.

Shear Cracks at Early Stages. In the square columns subjected to uniaxial loading: Series SS-0, the first shear cracks appeared around the lines through the compression corners at the top and bottom of column with the inclination of about 45° to the longitudinal axis of column, and extended out as to form flexure-shear cracks shown by A-C in Fig. 4(a). These cracks were intersected by the cracks due to the reverse loading. In the case of the square columns subjected to biaxial lateral loading: Series SS-45, the shear cracks appeared around the lines inclined at about 45°, but these cracks were not intersected by reverse cracks because the crack lines extended separately toward the protruding corner on both sides of column shown by B-D and B-D' in Fig.4(b). In the rectangular column SR-0-N1, with the least shear span ratio subjected to uniaxial lateral loading, the shear cracks appeared as diagonal tension cracks at an early stage. In the other rectangular columns, the features of initial shear cracking were rather similar to those of the square columns.

Failure Modes. As to the columns, either square or rectangular in cross section, under uniaxial lateral loading, the tendency was observed that the crack patterns until the ultimate stage transformed from flexure-shear cracks into more obvious diagonal tension cracks as the axial load was higher or shear span ratio was smaller. In the square columns subjected to biaxial

lateral loading, according as the skew angle of the lateral loading direction was closer to 45° and the effective shear span ratio was smaller, the cracks occurred diagonally but dispersed intermittently and their length became short. In the square columns with skew angle of 45°, the concrete cover over the longitudinal bars at the corner in mid-depth of both sides went to spall, and bond-splitting cracks along the corner at the extreme edge was induced under high axial load. In the rectangular column R-30-N1, under biaxial loading at 30° to the longer side of cross section, the displacement occurred in the direction of about 45° to the longer side and cracks appeared remarkably around the diagonal through the adjacent side faces (e and f in Fig. 3). In the case of SR-60-N1 under skew loading at an angle 60°, the displacement occurred in the direction with about right angle to the longer side and cracks on the shorter side faces (g in Fig.3) became severe like SR-90-N1 though cracks appeared on the longer side faces (h in Fig.3) were moderate.

SHEAR STRENGTH

Initial shear cracking stress and ultimate strength measured in the test are tabulated in Table 4 as compared with the calculated values. Calculated values for the columns subjected to uniaxial lateral forces are obtained from the equations described later on. Calculation for the columns subjected to biaxial lateral forces is based on the assumption that the normalized interaction curves are circles in the whole cases. Fig. 5(a) and (b) show the comparison of the stresses measured in the specimens under the biaxial lateral loading with the interaction cricles normalized by the stresses measured in the respective companion specimens loaded in the directions of both the two principal axes of cross section, at the initial shear cracking and ultimate, respectively. Each plotted mark represents the mean of absolute values of the positive and negative stresses at the specified stage. In each of these figures the data of square column specimens are plotted twice at the symmetric positions with respect to the line of 45° to the abscissa.

Equations for Shear Resistance. The following empirical equations for the shear strength of reinforced concrete beams were derived by K. Ohno and T. Arakawa in 1960 on the basis of the test results on the 156 restrained beams which represented the stress distribution in beams in building frames subjectd to lateral loads. (The expressions of Eq.(1) and (2) are altered from the originals for the convenience of use).

Initial shear cracking stress for beams;

$$_{0A}V_{sc} = k_c \frac{0.074\,(f'_c + 500)}{M/Vd + 1.70}\, b\, d \qquad (1)$$

Ultimate shear strength for beams;

$$_{0A}V_{su} = \left[k_u\, k_p \frac{0.10\,(f'_c + 180)}{M/Vd + 0.12} + 2.4\sqrt{p_w f_y}\right] b\, d \qquad (2)$$

where, k_c, k_u = coefficient for size of beam, (shown in Fig.7);
k_p = coefficient for logitudinal reinforcement ratio, (do.);
f'_c = compression strength of concrete, ⟨kg/cm²⟩;
M = the largest bending moment in referring span, ⟨kg-cm⟩;
d = effective depth of beam, ⟨cm⟩;
b = width of beam, ⟨cm⟩;
p_w = transverse reinforcement ratio;
f_y = yield stress of transverse reinforcement, ⟨kg/cm²⟩;
(Equation (2) should be unsuitable for simply supported beam, for which another equation was proposed).

The design provisions for shear in the Standard of Architectural Institute of Japan were obtained from conservative modification of these equations. By reconstructing the equations on the basis of the test results of about 130 restrained columns (loaded in double curvature) reported in Japan, the following equations for the shear resistance of columns were proposed by K. Ohno, T. Shibata and T. Hattori in 1972.

Initial shear cracking stress for columns:

$$ {}_{OSH}V_{sc} = \left(1 + \frac{\sigma_0}{150}\right) {}_{OA}V_{sc} = \left(1 + \frac{\sigma_0}{150}\right) \cdot k_c \frac{0.074\,(f'_c + 500)}{M^*/Vd + 1.70}\, bd \qquad (3) $$

Ultimate shear strength for columns:

$$ {}_{OSH}V_{su} = \left(0.9 + \frac{\sigma_0}{250}\right) {}_{OA}V_{su} = \left(0.9 + \frac{\sigma_0}{250}\right) \left[k_u\, k_p \frac{0.10(f'_c + 180)}{M^*/Vd + 0.12} + 2.4\sqrt{p_w f_y}\right] bd \qquad (4) $$

where, $\sigma_0 = P/bh$ = nominal axial stress, ⟨kg/cm²⟩;

P = axial load for column, ⟨kg⟩;

k_c, k_u = above-mentioned coefficients, (for columns in structures cast in-place or specimens cast in upright forms, $k_c = k_u = 1.0$ because the coefficients are to compensate bond loss on horizontally positioned longitudinal bars);

M^* = bending moment at the end of clear height of column.

Fig.8 (a) and (c) show the statistical comparison of the basic data with the calculated values by Eq.(3) and (4). The same data compared with the calculated values by the design equations in the Code of ACI in Fig.8(b) and (d).

Stress at Initial Cracking. In Fig.5(a) the plotted marks gather within the range of 20 % around the interaction circle. The ratios of the test values, ${}_tV_c$, to the calculated values, ${}_cV_c$, from Eq.(3) scatter from 0.64 to 1.08 as shown in Table 4. The mean of all the ratios is 0.91. It is generally inevitable that the deviation of cracking stresses is rather large because the conditions of occurrence and observation of the initial crack may be unsteady.

Ultimate Shear Strength. As shown in Fig.5(b), the normalized values of ultimate shear strength of the biaxially loaded specimens correspond with the circle assumed as the interaction curve. The ratios of the measured strength to the calculated strength from Eq.(4) scatter within the range of 0.82 to 1.21 as shown in Table 4 and the mean value of the ratios was 1.02. In Fig. 6, the ratios of the measured values to the calculated values are rearranged according to the skew angles of loading. As to square columns the ratio has a tendency to decrease as the skew angle is larger. In the case of rectangular columns, the ratio increases together with the angle of loading direction from longer side of cross section. The effect of axial load is indistinct in the comparison between $\eta = P/bhf'_c = 0$ and 1/6 and the ratios in these cases are rather above unity, but in the case of $\eta = 1/3$ the ratios are about unity and less than those in the other two cases. These tendencies mean that the ratios of columns injured ultimately due to flexure-shear cracks, SS-0-N0, SS-0-N1 and SR-90-N1, are higher than those of columns failed with diagonal tension cracks. The obvious differences between the conditions in the present test and those in the basic tests of the Eq.(4) are: (1) the whole specimens in the present test were subjected to repeated loading reversals, but in the latter tests only a few specimens were loaded in such manner; (2) the specimens in the present test provided intermediate vertical reinforcement, but no specimen provided them in the latter tests; excepting the loading methods. As to the former, it should be necessary to accumulate more test data. As to the latter, this may be considered as a problem with the effect of longitudinal reinforcement on shear strength. In Eq.(4) the effects of the longitudinal

reinforcement are entirely represented by the coefficient 'k_p' which is given as a function of tension reinforcement ratio 'p_t'. In the above comparison, the longitudinal bars in the face of tension side only were taken into account for 'p_t'. In the specimens with occurrence of conspicuous flexure-shear cracks, however, the intermediate longitudinal bars should be in tension zone and assist to increase the compression zone or to detain the decay of the compression zone at the critical section and consequently contribute to shear strength. Of course, the increase in dowel action should be counted up. Concerning the specimens: SS-0-N0, SS-0-N1 and SR-90-N1, as revising the ratio 'p_t' to include the intermediate bars and calculating the shear strength again, the calculated values became so similar to measured values as shown with the mark 'O' in Table 4. The scattering of the ratios of the measured values to the calculated values in the whole specimens became 0.82 to 1.13 and the mean of the ratios in the whole specimens changed to 1.00 Naturally, because the use of 'k_p' based on the bars in the face of tension side only is conservative, such usage for the convenience should be permitted.

DEFORMATION

Skeleton Curves. Fig. 9 shows an example of the relationship between shear stress and rotation of column. Fig. 10 shows skeleton curves of stress-rotation relationship in all the specimens. The yield points may be observed on the skeleton curves with a few exceptions though longitudinal reinforcement in most specimens never reached to the yield stress even at ultimate. It was confirmed that the yield points on skeleton curves corresponded to the occurrence of yield in transverse reinforcement. The skeleton curves in square columns were similar to one another in shape, or in characteristics at each of the levels of axial load regardless of the direction of lateral loading (Fig.10(a),(b)and(c)). In the rectangular columns, though the level of axial load was constant, the shape of skeleton curve varied according as the angle of the lateral loading direction to the longer side of cross section altered from 0° to 60°, except angles of 60° to 90° where the skeleton curves did not vary with the loading direction (Fig.10(d)).

Strain in Reinforcement. In the specimens subjected to no axial load: SS-0-N0, SS-45-N0 and SS-22.5-N0, transverse and longitudinal reinforcement resulted in yield nearly simultaneously at the time of appearance of yield on the skeleton curves. In the specimens subjected to axial load (marked as -N1 and -N2), only shear reinforcement went to yield corresponding to yield on the skeleton curves, while longitudinal reinforcement remained still below the yield point at yielding on skeleton curves. In a few specimens, a part of longitudinal bars reached to yield around the end of column at or after ultimate. Fig.11 and 12 show an example of the extending process of yielding in transverse reinforcement as correlated with proceeding of deformation of column (SS-45-N1). In this case , the stiffness of column decreased suddenly due to yielding of transverse bars. Yielding of transverse bars initiated at midheight of the column during the 7th cycle of lateral loading and dispersed upward and downward with increase of deformation of the column as the lateral load was descending after ultimate. The longitudinal bars reached to yield at the end of column (joint face) once during the 8th cycle (the ultimate strength) and came back below yield point in strain after the 10th cycle. The yield zone along bars was limited to less than about 10 cm from the end face. In the descending region after the ultimate strength the strain in the longitudinal bars decreased with the increase of deformation of column naturally,

but in contrast to the behavior of transverse reinforcement. Fig.13 shows the strain distribution in transverse reinforcement in the specimens: SS-0-N1 and SS-45-N1. Both of them are equal in shape and size of column and applied axial load but direction of lateral loading. In the test results they are nearly equal in cracking stress, ultimate strength and skeleton curve. However, they are remarkably different to each other in crack pattern. In the case of the specimen SS-0-N1, cracked in flexure-shear pattern under the uniaxial lateral loading, two peak values of strain in the transverse bars in the face of column along the loading direction appeared in the parts apart from both column ends by a half of column depth before yield. After yield occurred, the position of peak values of strain shifted to the parts apart from the column ends by unity of column depth. Strain in the transverse bars at midheight of the column remained to be small and never went to yield. The action of the transverse bars in the face perpendicular to the loading direction was a little through the test. In the specimen SS-45-N1 under the biaxial lateral loading, cracked in diagonal tension pattern, the peak values of strain in the transverse bars appeared in the parts of the tension side due to bending apart from the column ends by unity of column depth. After yield occurred, strain value increased rapidly around the midheight of column. The transverse bars in this part of all four faces went over the yield point.

CONCLUSIONS

Thirteen reinforced concrete column specimens with square or rectangular cross sections were subjected to biaxial lateral cyclic forces to study the shear strength, stress-deformation relationship and behavior of reinforcement under such loading conditions. On the basis of the test results, the following conclusions can be made:

1. The columns which will go to failure in flexure-shear mode under uniaxial lateral loading may often result in diagonal tension failure under biaxial lateral loading, because the ratio of height to depth of column becomes smaller in biaxial loading than that in uniaxial loading. Therefore, it is necessary to be cautious in saving transverse reinforcement in midheight of columns.

2. The normalized interaction curve for biaxial shear can be approximately expressed with an arc of circle, for ultimate shear strength as well as for initially shear cracking stress regardless of axial load intensity ($P/bhf'_C \leqq 1/3$) or shape of cross section.

3. By use of Eq.(3) for shear cracking stress and Eq.(4) for ultimate shear strength of columns, shear resistance of columns to lateral forces in any direction can be assessed with a good approximation.

4. Longitudinal reinforcing bars in the intermediate part of the actual depth of column in loading direction may be effective to increase the shear strength in direction concerned.

REFERENCES

1. Joh, O., Shibata, T., "Behaviors of R/C Rectangular Columns under Biaxial Bending Shear Reversals," Reports of Hokkaido Branch of AIJ, No.54, 1981.
2. Joh, O., Shibata, T., et al., "Failure of R/C Short Columns under Biaxial Bending Shear Reversals," Reports of Hokkaido Branch of AIJ, No.55, 1982.
3. Arakawa, T., "Shear Resistance of R/C Beams," Trans. of AIJ, No.66, 1960.
4. Hattori, T., Shibata, T., Ohno, K., et al., "Shear Strength and Deformability of R/C Columns," Proc. of Annual Meeting of AIJ, 1972.

Table 1 Combination of variables

	SS-0	SR-0	SR-90
Cross section (cm)	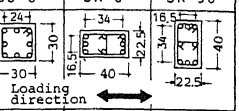		
$b \times h$	30x30	22.5x40	40x22.5
Longi. reinf.	8-D19 (p_g=2.25%)		
M/Vh	1.5	1.125	2.0
p_w(%) @(mm)	0.284 2-6φ @63	0.337 2-6φ @71	0.285 3-6φ @71

Table 2 Dimensions of specimens

Cross sect.	Loading direction	Axial load ratio	Mark of specimen
[cm] Square (SS) 30x30	θ=0°	η= 0	SS- 0 -N0
		1/6	SS- 0 -N1
		1/3	SS- 0 -N2
	θ= 22.5°	η= 0	SS-22.5-N0
		1/6	SS-22.5-N1
		1/3	SS-22.5-N2
	θ=45°	η= 0	SS-45-N0
		1/6	SS-45-N1
		1/3	SS-45-N2
Rect. (SR) 40x 22.5	θ=60°90° 30° 0°	η=1/6	SR- 0 -N1
			SR-30-N1
			SR-60-N1
			SR-90-N1

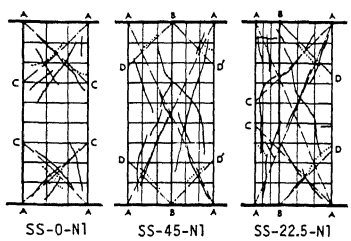

(-------initial stage, ——ultimate stage)

Fig.4 Typical cracks

Table 3 Properties of reinforcement

	Longi. reinf. D-19	Transv. reinf. 6φ
A (cm²)	2.87	0.269
σ_y (kg/cm²)	3980	3130
σ_B (kg/cm²)	6060	4000
ε (%)	19.9	31.0

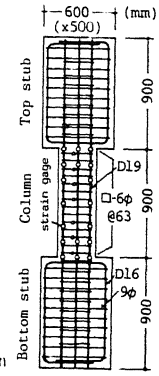

Fig.1 Test specimen

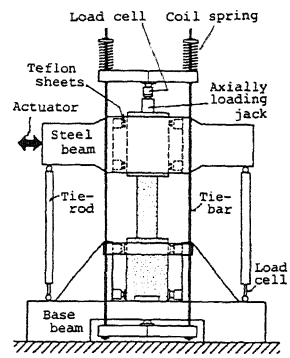

Fig.2 Loading arrangement

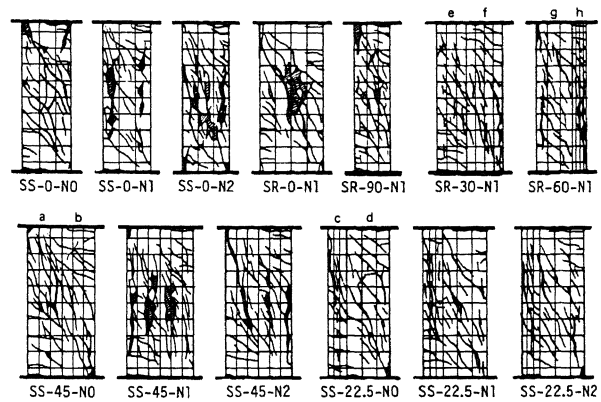

Fig.3 Crack patterns at final stages (except cracks in each reversing stage of half cycle)

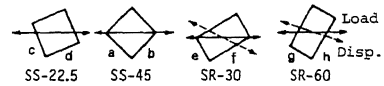

Table 4 Strength by measurement and calculation (unit=ton)

		Reversing stage	Initial shear cracking stress cVc	cVc	cVc/cVc	Ultimate shear strength tVu	cVu	tVu/cVu	f'_c kg/cm²
Uniaxial loading	SS- 0 -N0	+	11.1	13.2	0.84	21.0	19.6	1.07	234
		−	9.5	13.1	0.73	21.2	19.4	1.09	
	SS- 0 -N1	+	15.5	16.5	0.94	26.5	22.8	1.16	238
		−	16.6	16.5	1.01	25.9	22.8	1.14	
	SS- 0 -N2	+	20.1	19.6	1.03	26.8	25.6	1.04	237
		−	20.0	19.8	1.01	25.4	25.8	0.98	
	SR- 0 -N1	+	12.6	19.5	0.65	24.4	29.8	0.82	241
		−	17.2	19.5	0.88	27.1	29.6	0.91	
	SR-90-N1	+	13.1	13.6	0.96	21.9	18.4	1.19	253
		−	12.7	13.5	0.94	22.1	18.3	1.21	
Biaxial loading	SS-45-N0	+	13.1	13.9	0.94	20.5	20.8	0.98	274
		−	13.5	13.8	0.98	20.4	20.6	0.99	
	SS-45-N1	+	16.0	16.5	0.97	26.3	23.2	1.13	242
		−	17.3	16.6	1.05	24.7	22.8	1.08	
	SS-45-N2	+	20.8	20.3	1.02	26.2	26.9	0.97	264
		−	20.1	20.2	0.99	25.3	26.8	0.94	
	SS-22.5-N0	+	10.6	13.0	0.81	21.4	19.2	1.12	228
		−	9.1	13.0	0.71	20.0	19.1	1.04	
	SS-22.5-N1	+	16.0	16.0	1.00	23.4	22.2	1.05	223
		−	16.6	16.1	1.03	22.6	22.1	1.02	
	SS-22.5-N2	+	21.5	20.0	1.08	26.2	26.6	0.98	252
		−	21.0	19.9	1.06	25.8	26.4	0.98	
	SR-30-N1	+	15.6	18.0	0.87	24.7	26.2	0.94	256
		−	16.6	18.1	0.92	24.2	26.1	0.93	
	SR-60-N1	+	10.9	16.6	0.66	21.0	23.6	0.89	268
		−	11.5	16.7	0.69	21.5	23.4	0.92	

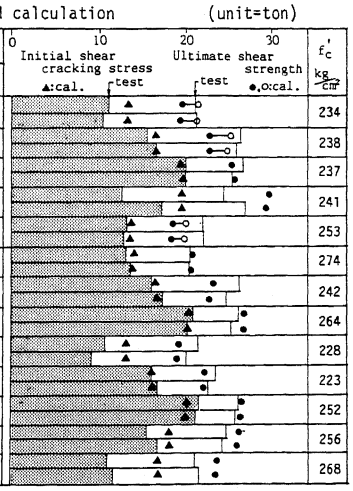

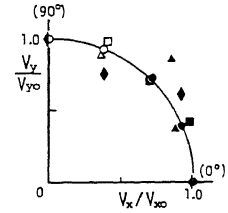

(a) cracking stress

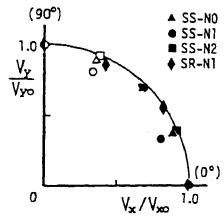

(b) Ultimate strength

Fig.5 Shear interaction

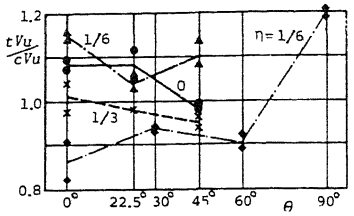

Fig.6 Ratios of measured value to calculated ultimate strength

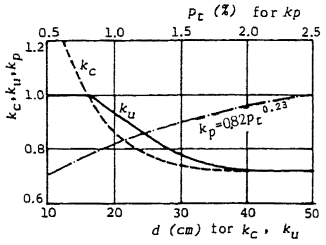

Fig.7 k_c, k_u, k_p

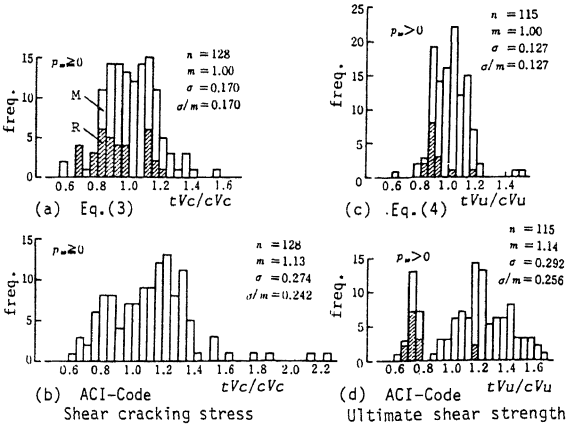

Fig.8 Distribution of test values versus calc. values

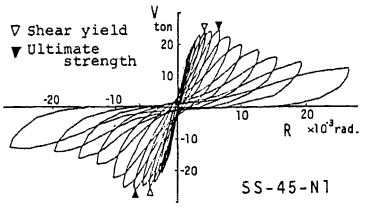

Fig.9 Shear-rotation relationship

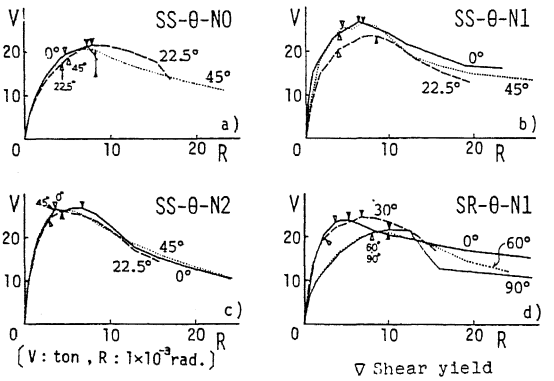

Fig.10 Skeleton curves

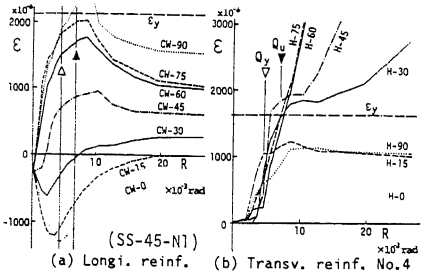

Fig.12 Strain-deformation relationship

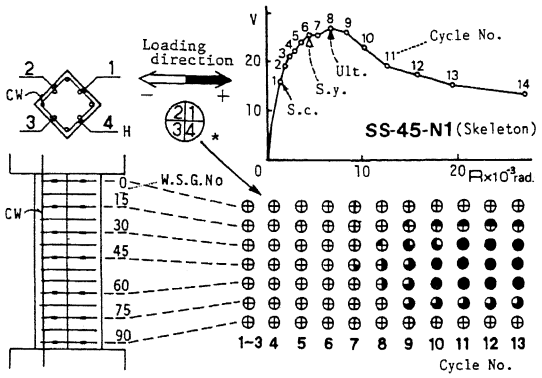

Fig.11 Process of yielding in transversed reinforcement

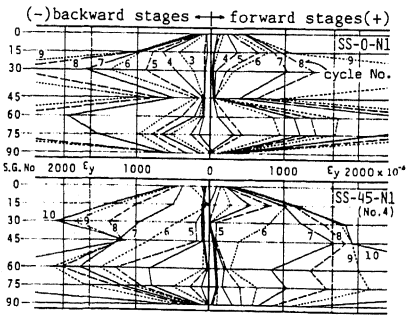

Fig.13 Strain distribution in transversed reinforcement